Photoionization in the presence of circularly polarized fundamental and odd-order harmonic fields

I. A. Ivanov,[1,3,*] Chang Hee Nam,[1,2] and Kyung Taec Kim[1,2,†]

[1]*Center for Relativistic Laser Science, Institute for Basic Science, 123 Cheomdangwagiro, Buk-gu, Gwangju 61005, Korea*

[2]*Department of Physics and Photon Science, GIST, Gwangju 61005, Republic of Korea*

[3]*Research School of Physics and Engineering, The Australian National University, Canberra, Australian Capital Territory 0200, Australia*

(Received 2 March 2017; revised manuscript received 3 April 2017; published 3 May 2017)

We present a study of the photoelectron spectra for the ionization process driven by counterrotating and corotating circularly polarized fundamental and odd-order harmonic fields. The main features of the spectra, such as symmetric lobed structures, are understood using simple arguments based on the strong field approximation (SFA) picture of ionization. A deviation from this picture is, most notably, the presence of the low-energy structures (LES) in the spectra. We show that the Rydberg states populated as a result of the combined absorption of the photons from the fundamental and harmonic fields are responsible for the origin of LES.

DOI: 10.1103/PhysRevA.95.053401

I. INTRODUCTION

Strong field ionization process driven by two circularly polarized laser pulses has recently received considerable attention in the literature [1–4]. The interplay of the two fields leads to the presence of unusual structures in the photoelectron spectra, such as helical vortex structures [4] for ionization by two counterrotating pulses of the same frequency, or symmetrical structures appearing in the case of a two-color ionization [1].

In the latter work a field configuration consisting of a circularly polarized fundamental field and its second harmonic (for both counterrotating and corotating geometries) was used. It was shown that the general features of the photoelectron spectra for these field configurations generally agree with the expectations based on the standard strong field approximation (SFA) theory [5–7]. In particular, the photoelectron spectrum for this field configuration exhibits a three-lobed structure for the counterrotating, and a single-lobed structure for the corotating case. It was found also that this field configuration offers a possibility to study and control, to some extent, the rescattering process [1], and thus study separately the tunneling and rescattering steps, which are important ingredients for the genesis of many phenomena accompanying strong-field ionization.

A manifestation of this control over the rescattering process which this field configuration consisting of the fundamental field and its second harmonic allows to achieve, were the low-energy structures (LES) in the photoelectron spectra which were shown to be present in the counterrotating and absent in the corotating field geometries [1]. Since one of the mechanisms of the appearance of LES is a process of rescattering [8–11], and classical rescattering trajectories are known to exist only for the counterrotating case, it was shown unambiguously that the LES in this case were due to the rescattering process. In another work [2] it was found that for the counterrotating fundamental field and its second harmonic a significant increase of the nonsequential double-ionization yield can be achieved.

A natural generalization of this setup would be a field configuration consisting of the circularly polarized fundamental field and its higher harmonics. We will present below a theoretical study of the ionization process for such a configuration. The higher harmonics presently obtainable are considerably weaker than the fundamental field. We will consider, therefore, harmonic fields with field intensities one percent of the fundamental field. To some extent this choice limits the dynamics. Clearly, in this case we can have the classical rescattering trajectories neither for the counterrotating nor for the corotating geometries (the second harmonic field strength used by the authors of [1] was comparable to that of the fundamental field, thereby enabling the existence of the rescattering trajectories for the counterrotating geometry). Our choice of the ratio of the field intensities of harmonic and fundamental fields was motivated by the desire to use experimentally achievable pulse parameters. We will see, nevertheless, that even in the absence of the rescattering process, ionization for this field geometry presents some interesting and puzzling features, in particular, the presence or absence of LES for different choices of the field geometry (though the mechanism leading to the appearance of the LES in this case is not the rescattering, but a different process as to be explained below). Atomic units are used throughout the paper.

II. THEORY

A. Solution of the TDSE

We solve the time-dependent Schrödinger equation (TDSE) for a hydrogen atom in the presence of a laser pulse as follows:

$$i\frac{\partial\Psi(\boldsymbol{r})}{\partial t} = [\hat{H}_{\rm atom} + \hat{H}_{\rm int}(t)]\Psi(\boldsymbol{r}). \tag{1}$$

We use velocity form for the operator $\hat{H}_{\rm int}(t)$ describing the interaction of the atom with the laser field

$$\hat{H}_{\rm int}(t) = \boldsymbol{A}(t)\hat{\boldsymbol{p}}, \tag{2}$$

where $\boldsymbol{A}(t) = -\int_0^t \boldsymbol{E}(\tau)\,d\tau$ is the vector potential of the field configuration we consider, which is defined in terms of the

*Igor.Ivanov@anu.edu.au

†kyungtaec@gist.ac.kr

electric field components as follows:

$$E_x(t) = \frac{f(t)}{\sqrt{2}}(E_1 \cos\omega t + E_q \cos q\omega t),$$
$$E_y(t) = \frac{f(t)}{\sqrt{2}}(E_1 \sin\omega t \pm E_q \sin q\omega t), \quad (3)$$

where, in the second of these equations we should use the minus sign for the counterrotating and the plus sign for the corotating geometry. The field strength of the fundamental field is $E_1 = 0.0534$ a.u., corresponding to the intensity of 10^{14} W/cm^2. As mentioned above, the harmonic field strength was chosen as $E_q = E_1/10$. The results of the calculations for $q = 3$ and $q = 5$ are reported below. The function $f(t) = \sin^2(\pi t/T_1)$ in Eq. (3) is a pulse envelope $T_1 = NT$ where integer N is a total pulse duration (the particular values used in the calculations were $N = 12$ for $q = 3$ and $N = 10$ for $q = 5$), $T = 2\pi/\omega$ is an optical cycle corresponding to the fundamental frequency $\omega = 0.0577$ a.u. (wavelength of 790 nm).

The initial state of the system is the ground state of a hydrogen atom. To solve the TDSE we employed the procedure described in the works [12–14]. The solution of the TDSE is represented as a series in spherical harmonics

$$\Psi(\boldsymbol{r},t) = \sum_{l,m} f_l(r,t) Y_l^m(\theta,\phi), \quad (4)$$

where spherical harmonics with orders up to $L_{\max} = 50$ were used. The radial variable is treated by discretizing the TDSE on a grid with the step-size $\delta r = 0.1$ a.u. in a box of the size $R_{\max} = 1000$ a.u. Necessary checks were performed to ensure that for these values of the parameters $L_{\max}$ and $R_{\max}$ the convergence of the calculations has been achieved. The wave function $\Psi(\boldsymbol{r},t)$ was propagated in time using the matrix iteration method [15].

B. Distribution of photoelectrons

Electron momentum distributions were found by projecting the calculated wave function $\Psi(\boldsymbol{r},t)$ after the end of the pulse on the set of the (ingoing) scattering states of the hydrogen atom. General features of the photoelectron spectrum for the field configurations we consider can be inferred from the simple SFA picture of ionization, in which ionization occurs at the times t_m of the peak field strength of the pulse, with the final electron velocity given by the value of the vector potential at this moment of time. Assuming for simplicity that the pulse envelope is flat (which is a good enough approximation for the sufficiently long pulses we consider), and considering the counterrotating geometry, one can easily see that the total electric field of the pulse has $q + 1$ peak values of equal magnitude per each cycle of the fundamental field at times $t_m = \frac{mT}{q+1}$ $(m = 0, \ldots, q)$, with vector potential components

$$A_x(t) = -\frac{E_1}{\omega\sqrt{2}}\left(1 - \frac{C}{q}\right)\sin\omega t_m\ ,$$
$$A_y(t) = \frac{E_1}{\omega\sqrt{2}}\left(1 - \frac{C}{q}\right)\cos\omega t_m\ . \quad (5)$$

Here $C = \frac{E_q}{E_1} = 0.1$. According to this simple picture, for the counterrotating geometry the photoelectron spectra should form a regular structure with $q + 1$ lobes in the polarization plane of the pulse. For the case of the corotating circularly polarized fundamental field and its qth harmonic a simple analysis proceeds analogously, with the result that the photoelectron spectra in this case should exhibit a structure with $q - 1$ lobes in the polarization plane of the pulse.

III. RESULTS AND DISCUSSION

Photoelectron momentum distributions in the polarization plane are shown in Fig. 1 for the counterrotating fundamental and third (left panel of the figure) and fifth (right panel) harmonics. We present results given by the TDSE calculation described above and the results given by an SFA calculation. For the field geometry we consider, SFA ionization amplitude for a hydrogen atom can be written, following the well-known prescriptions of the SFA theory [16,17], as (we use velocity gauge)

$$a_{\boldsymbol{p}} = -i\int_0^{T_1} g(t,\boldsymbol{p}) \exp\left\{\frac{i}{2}\int_0^t [\boldsymbol{p} + \boldsymbol{A}(\tau)]^2\, d\tau - i\varepsilon_0 t\right\} dt, \quad (6)$$

with $g(t,\boldsymbol{p}) = (\boldsymbol{A}(t)\boldsymbol{p} + \frac{A^2(t)}{2})\frac{\sqrt{2}}{\pi(1+p^2)^2}$, where $\varepsilon_0 = -0.5$ a.u. is the ground-state energy of the hydrogen atom, annd $\boldsymbol{A}(t)$ is the vector potential for our field configuration which we compute as $\boldsymbol{A}(t) = -\int_0^t \boldsymbol{E}(\tau)\, d\tau$ using expressions (3) for the electric fields.

Both the TDSE and SFA spectra shown in Fig. 1 exhibit the $q + 1$-lobed structure in agreement with the simple picture encapsulated by Eq. (5). The momentum distributions given by the TDSE calculation are rotated, as a whole, relative to the SFA distributions. That is, of course, an expected feature. The Coulomb interaction, totally neglected in the simplest version of the SFA described by the Eq. (6), is responsible for the rotation of the spectra producing the Coulomb correction to the observed offset angle [18], a well-known effect which must be taken into account for the correct interpretation of the experimental [19] or theoretical [18] applications of the angular attosecond streaking technique. A most notable departure from the prediction of the SFA, clearly manifest in Fig. 1, is the low-energy structure (LES) visible in the central part of the $q = 5$ case. Before discussing the possible origin of this structure, we will present some other results which this discussion will necessitate.

In Fig. 2 we show the results of the calculation for the corotating fundamental and fifth harmonic. The pulse parameters we used in this calculation are the same used above for the counterrotating geometry. Figure 2 shows spectrum possessing a $q - 1$-lobed symmetry as prescribed by the simple SFA analysis we made above. We may also note the absence of the LES in this case. The calculation for the $q = 3$ case which we performed (we do not report the results here because they do not provide essentially new information) shows, as expected, a two-lobed structure and the absence of the LES.

On the basis of the findings presented in Figs. 1 and 2 the origin of the LES for the $q = 5$ case appears unclear. It is a

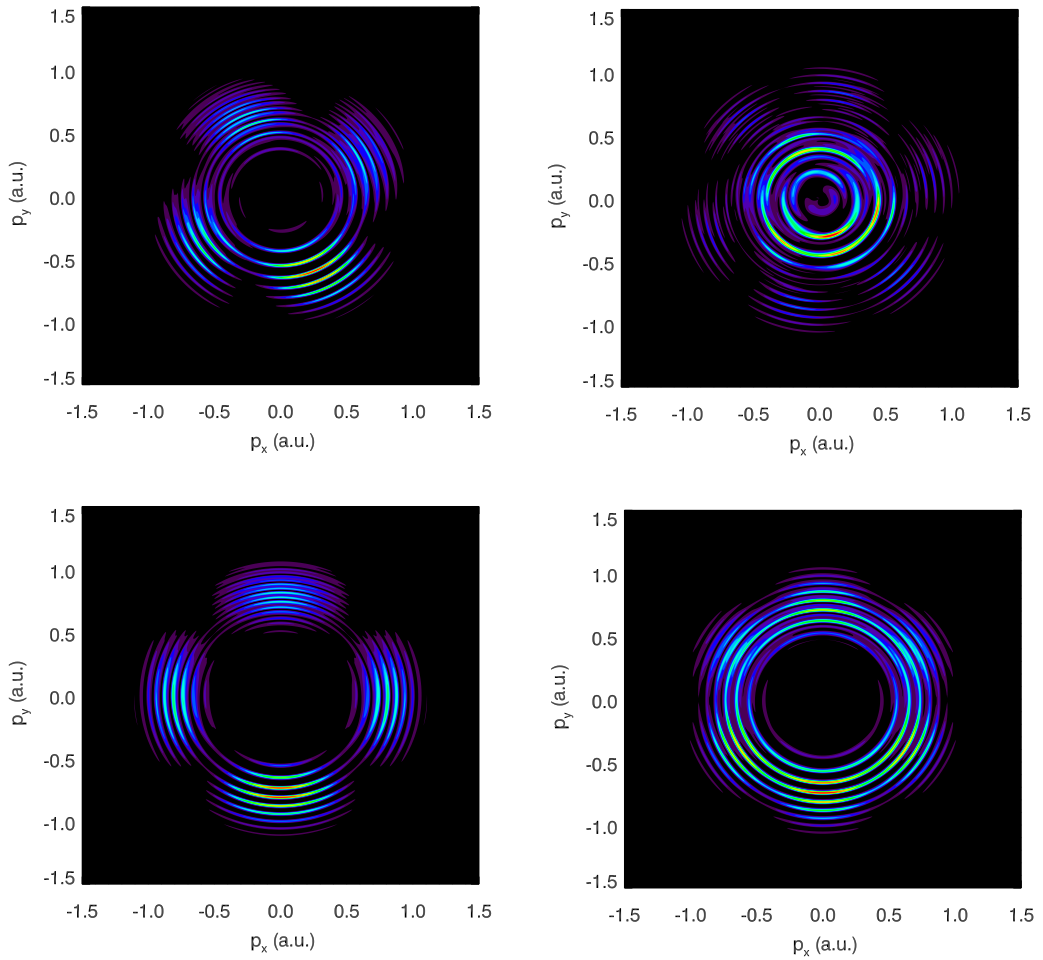

FIG. 1. Ionization probability distribution in the polarization plane for the counterrotating fundamental and third harmonic (left panel), and fundamental and fifth harmonic (right panel) fields given by the TDSE (first row) and SFA (second row) calculations based on Eq. (6). Pulse parameters: intensity and frequency of the fundamental field are $I = 10^{14}$ W/cm^2, $\omega = 0.057$ a.u. (wavelength of 790 nm). Intensities of the third and fifth harmonics were 10^{12} W/cm^2.

well-known fact [8,20,21] that LES, which are not predicted by the ordinary SFA, can be present in the electron spectra of different atomic targets for energies of the order of a fraction of the ponderomotive energy. The LES have been found to disappear with growing ellipticity of the driving laser pulse [20,22], which lead to a conclusion that a rescattering process is responsible for their origin [8]. For the circularly polarized fields we consider, however, the rescattering probability is very low. It is known that rescattering trajectories exist for the counterrotating geometry, and, consequently, the rescattering process may lead to a significant nonsequential double ionization probability [2]. These trajectories, however, exist only in the case of comparable field strengths of the counterrotating electric fields [1,2] and are clearly absent in the case of the ratio $E_q/E_1 = 0.1$ we used above in defining the electric field of the pulse. Moreover, for the weak harmonic field we consider, the classical trajectories (or even quantum trajectories which have also been used to explain LES [9,23]) should be essentially the same for both the $q = 3$ and $q = 5$ cases, regardless of the type (counterrotating or corotating) of the field geometry we employ.

An alternative mechanism, which may lead to the appearance of the low-energy electrons in the spectra, is the population trapping in the Rydberg states [22,24]. A useful insight into the role of this mechanism in our problem can be obtained by analyzing the distribution $P(E,m)$, where E is electron energy, m the projection of the electron angular momentum on the z axis [we use here geometry encapsulated in Eq. (3), where the (x,y) plane is a polarization plane of the laser pulse]. This distribution, giving a probability to detect in the final state an escaped electron with given energy and angular momentum projection, can be easily obtained from the TDSE calculation by projecting the solution of the TDSE after the end of the pulse on an appropriate set of the continuous spectrum states.

The shape of the distribution $P(E,m)$ is largely dictated by the well-known selection rules, which state in our case that the absorption of a photon from the fundamental field in Eq. (3) increases the electron angular momentum projection by one unit, while the absorption of a photon from the counterrotating harmonic field decreases it by one unit. $P(E,m)$ thus provides a complimentary, photon-based picture of the ionization process. Assuming that the electron absorbs M photons from the fundamental field and N photons from the counterrotating qth harmonic field, we have for the electron energy E and

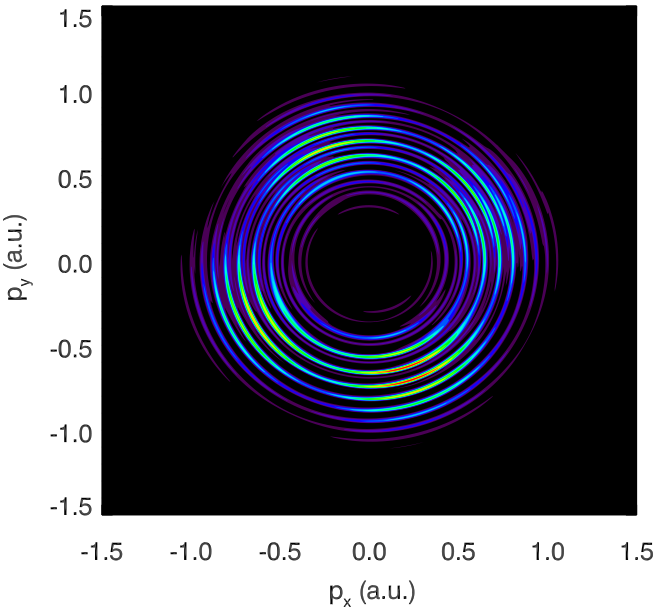

FIG. 2. Ionization probability distribution in the polarization plane for the corotating fundamental and fifth harmonic fields. Pulse parameters: intensity and frequency of the fundamental field are $I = 10^{14}$ W/cm^2, $\omega = 0.057$ a.u. (wavelength of 790 nm). Intensity of the fifth harmonic: 10^{12} W/cm^2.

angular momentum projection m in the final state

$$\frac{E}{\omega} = M + qN - \frac{I_p + U_p}{\omega}, \qquad m = M - N, \tag{7}$$

where U_p is the ponderomotive energy, $I_p = 0.5$ a.u. the ionization potential of the hydrogen atom. From Eq. (7) we obtain

$$\frac{E}{\omega} = m + (q+1)N - \frac{I_p + U_p}{\omega}\,. \tag{8}$$

According to this equation, for a fixed number N of absorbed harmonic photons, the most probable electron energy E is a linear function of the momentum projection m. The maxima of the distribution $P(E,m)$ must then, for a fixed N, lie on a line $E = m\omega + N(q+1)\omega - I_p - U_p$, producing a band in the (E,m) plane. We may have several parallel bands corresponding to different numbers of the absorbed harmonic photons.

Figure 3 shows calculated $P(E,m)$ distributions for $q = 3$ and $q = 5$ cases (counterrotating geometry). The tilted bands, corresponding to different numbers of absorbed harmonic photons N, are clearly visible in Fig. 3, in agreement with the expectations based on the simple arguments we gave above. From Eq. (8) we obtain $N = [(I_p + U_p)/\omega - m_0]/(q+1)$, where m_0 is the value of m for which a tilted band crosses the horizontal axis. Using $U_p = E_1^2/2\omega^2$ for the pulse in Eqs. (3) and estimating values of m_0 from Fig. 3 as $m_0 \approx 5$ for both $q = 3$ and $q = 5$, we obtain $N = 2$, $M = 7$ for the most prominent tilted band in Fig. 3 for the case $q = 5$ and $N = 3$, $M = 8$ for the case $q = 3$. From the point of view of the photon picture, therefore, the most probable ionization channel for $q = 5$ is characterized by the absorption of two harmonic photons, while it is the absorption of three harmonic photons for the case of $q = 3$. It is clear, therefore, why we have no LES for the case of $q = 3$, it is generally a higher order (with respect to the harmonic field), and consequently weaker process.

To elucidate further the picture of the ionization process, we will take a closer look at the role which Coulomb interaction may play in producing observed behavior. In Fig. 4 we show results obtained if we solve TDSE for the Yukawa potential $V(r) = e^{-0.1r}/r$ for the same field geometries we used above.

Both photoelectron and $P(E,m)$ distributions shown in Fig. 4 show the absence of LES. This agrees with the findings reported in [24], where it was shown that even a small screening parameter suppresses LES. Another feature manifest in Fig. 4 is the absence of a significant additional offset from the positions of the maxima of the momentum distribution predicted by the SFA-based Eq. (5), which was present in the Coulomb case. This was to be expected, as this additional offset is a signature of the Coulomb interaction. The fact that LES are absent in the case of the Yukawa potential hints that the LES

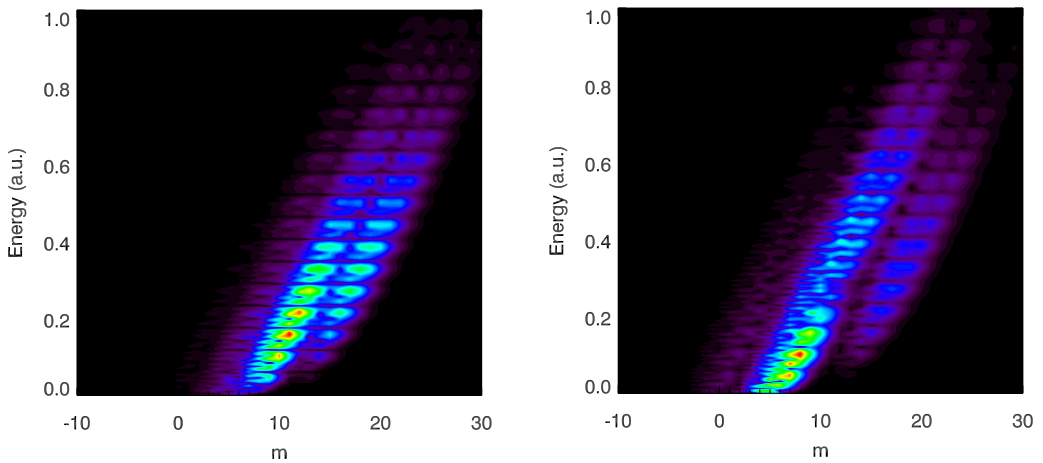

FIG. 3. $P(E,m)$ (energy, momentum projection) distribution for the counterrotating fundamental and third harmonic (left panel), and fundamental and fifth harmonic (right panel) fields. Pulse parameters: intensity and frequency of the fundamental field are $I = 10^{14}$ W/cm^2, $\omega = 0.057$ a.u. (wavelength of 790 nm). Intensities of the third and fifth harmonics were 10^{12} W/cm^2.

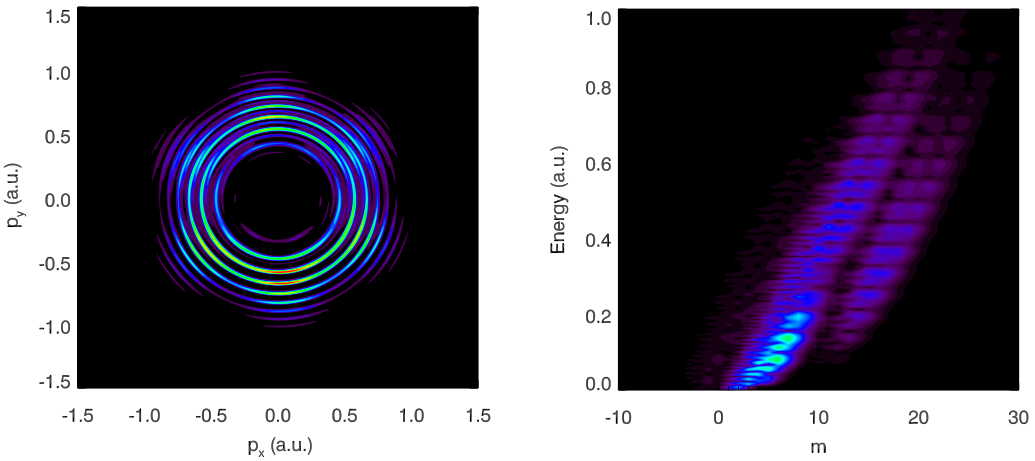

FIG. 4. Ionization probability distribution in the polarization plane for the counterrotating fundamental and fifth harmonic fields for the Yukawa potential (left panel), and $P(E,m)$ distribution (right panel) for this geometry. Pulse parameters: intensity and frequency of the fundamental field are $I = 10^{14}$ W/cm^2, $\omega = 0.057$ a.u. (wavelength of 790 nm). Intensity of the harmonic: 10^{12} W/cm^2.

in our case might be due to the presence of the rich structure of excited states which disappears with the introduction of a screening factor.

To confirm this suggestion we analyzed the distribution $P(m)$, which is the probability to find the system in a bound excited state with a given value of the angular momentum projection m after the end of the laser pulse. Mathematically, this distribution can be defined as

$$P(m) = \langle \Psi(T_1)|\hat{Q}(m)|\Psi(T_1)\rangle, \tag{9}$$

where $\Psi(T_1)$ is the TDSE wave function taken at the end of the laser pulse and

$$\hat{Q}(m) = \sum_{\substack{n,l \text{ for excited} \\ \text{states}}} |\phi_{nlm}\rangle\langle\phi_{nlm}| \tag{10}$$

is the projector on the set of all exited bound states with fixed m. Distributions $P(m)$ are shown in Fig. 5.

We see that the distribution for the counterrotating Coulomb case for $q = 5$ is peaked at $m = 4$. This fact suggests that LES in the spectrum for this case may arise as a result of the absorption of a photon of the fundamental field from the Rydberg states with $m = 4$. This agrees with the fact we established above, that the LES in the right panel of Fig. 1 are due to the electrons with angular momentum projection $m = 5$, which are produced by absorbing $M = 7$ photons from the fundamental and $N = 2$ photons from the harmonic field. The manifold of the Rydberg states with $m = 4$ from which these electrons escape into the continuum, therefore, is populated by absorbing $M = 6$ photons from the fundamental and $N = 2$ photons from the harmonic field. One may inquire why this particular combination of the fundamental and harmonic photons and the particular manifold of the Rydberg states with $m = 4$ play such an important role. We note first that using for the ponderomotive energy an estimate $U_p = E_1^2/2\omega^2 \approx 0.438$ a.u. (where E_1 is the field strength of the fundamental field), the energy of the electron absorbing energy of 16ω from the electromagnetic fields is ≈ -0.027 a.u., which is close to the energy of the manifold of the Rydberg states with $n = 5$. We may tentatively suppose, therefore, that it is this manifold of the Rydberg states which is responsible for the appearance of the LES. As far as the energy balance is concerned, this manifold can be reached by different pathways. Any integer solution to the equation $M + 5N = 16$ gives us a pair (M,N) of the number of absorbed fundamental and harmonic photons leading to the same Rydberg manifold with $n = 5$. Besides the solution $M = 6, N = 2$, which leads to the submanifold of the Rydberg states with $M = 4$ which we discussed above, there are possible solutions $M = 1, N = 3$ and $M = 11, N = 1$. Note, however, that solution $M = 1, N = 3$ corresponds to a higher (third) order process with respect to the absorption of harmonic photons, which for the weak harmonic field strength of 0.01 a.u. we consider has a smaller probability than the second-order process corresponding to the $M = 6, N = 2$

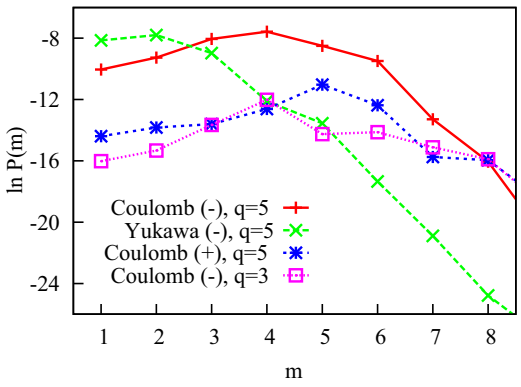

FIG. 5. Angular momentum projection distribution $P(m)$ of the population of the bound states (excluding the ground state) for the counterrotating fundamental and fifth harmonic fields for the Coulomb and Yukawa potentials, corotating fundamental and fifth harmonic fields (Coulomb potential), and the counterrotating fundamental and third harmonic fields (Coulomb potential). The cases are denoted in the figure legend as Coulomb $(-)$ $q = 5$, Yukawa $(-)$ $q = 5$, Coulomb $(+)$ $q = 5$, and Coulomb $(-)$ $q = 3$, respectively. Pulse parameters: intensity and frequency of the fundamental field are $I = 10^{14}$ W/cm^2, $\omega = 0.057$ a.u. (wavelength of 790 nm). Intensity of the harmonic field: 10^{12} W/cm^2.

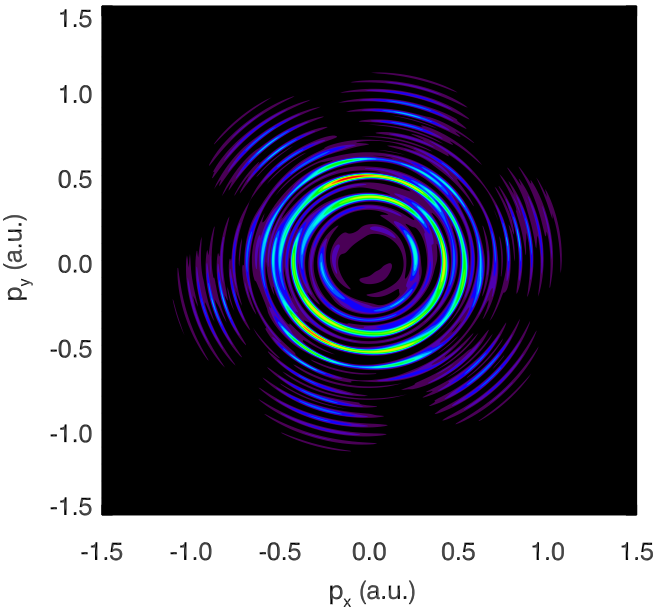

FIG. 6. Ionization probability distribution in the polarization plane for the counterrotating fundamental and fifth harmonic for the fundamental frequency of $\omega = 0.0547$ a.u. Other pulse parameters: intensity of the fundamental field $I = 10^{14}$ W/cm^2, intensity of the fifth harmonic 10^{12} W/cm^2.

pair. The photon absorption process corresponding to the pair $M = 11, N = 1$, on the other hand, cannot populate the manifold of the Rydberg states with $n = 5$ since it leads (due to the dipole selection rules) to the much higher value $m = 10$ of the projection of the electron angular momentum. There are no states with $m = 10$ in the manifold of the Rydberg states with $n = 5$.

The mechanism which we outlined above attributes LES to the resonance population of a certain manifold of the Rydberg states and must, consequently, have a resonance character exhibiting sensitivity to the photon frequency. We performed a separate calculation for the counterrotating geometry for $q = 5$ using a slightly different value ($\omega = 0.0547$) for the frequency of the fundamental field. The results are shown in Fig. 6. A comparison of this figure and the corresponding distribution in Fig. 1 shows that the LES in the spectrum for the $\omega = 0.0547$ a.u. case are considerably weaker than for $\omega = 0.0577$ a.u.

For the counterrotating case with $q = 3$ population of the Rydberg states with large m, which might produce LES is much lower. This is because Rydberg states in this case are populated by three harmonic photons (not two as in the $q = 5$ case), which for the harmonic fields of small intensity we consider is a much weaker process. Hence, the LES for the counterrotating case with $q = 3$ are suppressed. In the case of the Yukawa potential we do not have a Rydberg series at all, the m distribution sharply drops, and the LES are absent. An explanation of the absence of LES for the case of the corotating fields with $q = 5$ is similar to the one we gave above when discussing why the process corresponding to the pair $M = 11, N = 1$, though satisfying the energy balance, cannot populate the $n = 5$ manifold of the Rydberg states. The absorption of a pair (M, N) of the fundamental and harmonic photons leads for the corotating geometry (due to the dipole selection rules) to the electronic states with electron momentum projection $m = M + N$, while $m = M - N$ for the absorption of M fundamental and N harmonic photons for the counterrotating geometry. For M and N such that a group of the Rydberg states can be resonantly populated, the electronic states with angular momentum projection $m = M + N$ can, in fact, be absent in the particular manifold of the Rydberg states. This, we believe, happens in our problem. For example, the process corresponding to the pair $M = 6, N = 2$ would lead for the corotating geometry to the electronic states with $m = 8$ belonging to a higher-lying manifold of the Rydberg states, which is off-resonance. The LES, therefore, are not produced.

IV. CONCLUSION

We present a study of the photoelectron spectra for the ionization process driven by counterrotating and corotating circularly polarized fundamental and odd-order harmonic fields. The main features of the spectra, such as the symmetric patterns, can be easily explained using simple arguments based on the SFA theory of ionization. Relatively minor deviations from the SFA picture (the presence of the overall rotation of the spectra in the polarization plane, the so-called Coulomb offset angles) are well understood, and the result from the effect of the Coulomb interaction.

The main difference with the SFA predictions, which can be observed in the calculated photoelectron spectra, is the presence of the LES. Of all the field configurations we considered, LES were present only for the case of ionization driven by the counterrotating fundamental field and its fifth harmonic. LES were found neither for the corotating fundamental field and harmonic fields, nor for the case of the counterrotating fundamental field and its third harmonic. In the case of the counterrotating fundamental field and its fifth harmonic, LES were found to disappear if we used screened Coulomb potential in the calculations. We tried to elucidate this phenomenon, and found that the resonant population of the manifold of the Rydberg states with $n = 5$ by the process of a combined absorption of the photons from the fundamental and harmonic fields is responsible for its origin.

ACKNOWLEDGMENT

This work was supported by the Institute for Basic Science under IBS-R012-D1.

[1] C. A. Mancuso *et al.*, Phys. Rev. A **91**, 031402(R) (2015).
[2] J. L. Chaloupka and D. D. Hickstein, Phys. Rev. Lett. **116**, 143005 (2016).
[3] M. Richter, M. Kunitski, M. Schöffler, T. Jahnke, L. P. H. Schmidt, and R. Dörner, Phys. Rev. A **94**, 033416 (2016).

[4] J. M. Ngoko Djiokap, S. X. Hu, L. B. Madsen, N. L. Manakov, A. V. Meremianin, and A. F. Starace, Phys. Rev. Lett. **115**, 113004 (2015).
[5] L. V. Keldysh, Sov. Phys. JETP **20**, 1307 (1965).
[6] F. H. M. Faisal, J. Phys. B **6**, L89 (1973).
[7] H. R. Reiss, Phys. Rev. A **22**, 1786 (1980).
[8] H. H. M. Faisal, Nat. Phys. **5**, 319 (2009).
[9] T.-M. Yan, S. V. Popruzhenko, M. J. J. Vrakking, and D. Bauer, Phys. Rev. Lett. **105**, 253002 (2010).
[10] C. Liu and K. Z. Hatsagortsyan, Phys. Rev. Lett. **105**, 113003 (2010).
[11] A. Kästner, U. Saalmann, and J. M. Rost, Phys. Rev. Lett. **108**, 033201 (2012).
[12] I. A. Ivanov, Phys. Rev. A **90**, 013418 (2014).
[13] I. A. Ivanov and A. S. Kheifets, Phys. Rev. A **87**, 033407 (2013).
[14] I. A. Ivanov and A. S. Kheifets, Phys. Rev. A **89**, 021402 (2014).
[15] M. Nurhuda and F. H. M. Faisal, Phys. Rev. A **60**, 3125 (1999).
[16] S. V. Popruzhenko, J. Phys. B **47**, 204001 (2014).
[17] D. B. Milošević, G. G. Paulus, D. Bauer, and W. Becker, J. Phys. B **14**, R203 (2006).
[18] L. Torlina *et al.*, Nat. Phys. **11**, 503 (2015).
[19] P. Eckle, A. N. Pfeiffer, C. Cirelli, A. Staudte, R. Dörner, H. G. Muller, M. Büttiker, and U. Keller, Science **322**, 1525 (2008).
[20] C. I. Blaga, F. Catoire, P. Colosimo, G. G. Paulus, H. G. Muller, P. Agostini, and L. F. DiMauro, Nat. Phys. **5**, 335 (2009).
[21] W. Quan *et al.*, Phys. Rev. Lett. **103**, 093001 (2009).
[22] J. Dura *et al.*, Sci. Rep. **3**, 2675 (2013).
[23] W. Becker, S. P. Goreslavski, D. B. Milošević, and G. G. Paulus, J. Phys. B **47**, 204022 (2014).
[24] Q. Z. Xia, D. F. Ye, L. B. Fu, X. Y. Han, and J. Liu, Sci. Rep. **5**, 11473 (2015).